Int. J. Electrochem. Sci., 16 **(2021)** Article ID: 210249, doi: 10.20964/2021.02.42

International Journal of
ELECTROCHEMICAL
SCIENCE
www.electrochemsci.org

Biomass of Microalgae *Chlorella sorokiniana* as Green Corrosion Inhibitor for Mild Steel in HCl Solution

Gustavo Almeida de Oliveira[1], *Viviane Maia Teixeira*[1], *Jéssica Nogueira da Cunha*[1], *Matheus Rangel dos Santos*[1], *Victor Magno Paiva*[1], *Michelle Jakeline Cunha Rezende*[1], *Anita Ferreira do Valle*[1], *Eliane D'Elia*[1,*]

Federal University of Rio de Janeiro, Institute of Chemistry, University City, 21941-909, Rio de Janeiro, Brazil.
[*]E-mail: eliane@iq.ufrj.br

Received: 3 October 2020 / *Accepted:* 23 November 2020 / *Published:* 31 December 2020

Biomass of microalgae *Chlorella sorokiniana* was studied as a green inhibitor of corrosion of mild steel in 1 mol L^{-1} HCl solution. The investigation includes weight-loss experiments, potentiodynamic polarization curves, electrochemical impedance measurements and surface analysis by scanning electron microscopy. The use of 100 mg L^{-1} of the *Chlorella sorokiniana* biomass reached an inhibition efficiency of 94.6% after 24 h of immersion. The addition of the microalgae biomass did not change the apparent activation energy which characterizes adsorption by blocking, showing that the constituents form a protective film on the metallic surface of mild steel. The high molecular weight fraction isolated from the biomass showed an inhibition efficiency close to the total biomass, which suggests that proteins macromolecules are probably responsible for the inhibitory action observed by the microalgae biomass.

Keywords: mild steel, green inhibitor, microalgae *Chlorella sorokiniana*.

1. INTRODUCTION

Corrosion can be defined as the deterioration of metallic materials, by chemical or electrochemical action of the environment, associated or not to mechanical efforts, which lead to harmful changes, making the materials unsuitable for use [1]. Corrosion can cause significant damage to industry, either directly or indirectly, as well as accidents.

According to the National Association of Corrosion Engineers, the implementation of prevention strategies can reduce the cost of corrosion around 15–35%, which means a saving of USD 375–875 billion [2]. Thus, it is extremely important to develop technologies that reduce and mitigate the effects of corrosion. Currently, several methods have been studied and applied to prevent

corrosion, including corrosion inhibitors, protective coatings, and cathodic and anodic protection [3]. Corrosion inhibitors have been the most used method, with wide application in the industrial area. Corrosion inhibitors can be divided into two categories, organic and inorganic. Inorganic inhibitors, such as nitrite, nitrate, chromate, dichromate and phosphate salts, work by mitigating the cathodic or anodic reactions, while organic inhibitors, which are compounds containing one or more polar groups (with atoms of O, N, P, S and π electrons), act by a physical or chemical adsorption mechanism [4–5].

Although many of these compounds have high inhibition efficiency, they can cause undesirable effects, such as toxicity and they have a high cost. As a result, the demand for natural corrosion inhibitors (such as plants and algae) is growing, as they are biodegradable, do not contain heavy metals, have easy extraction or production, and are low cost [5–14]. Plant extracts represent a rich source of natural organic compounds that include heterocyclic alkaloids and flavonoids, polycyclic compounds, and cellulose, among others, which can contribute to the formation of a film on the metal surface, preventing corrosion and bringing environmental benefits [15–17].

Algae extracts are widely used in both the medical and aesthetic fields. Microalgae have considerable biotechnological potential and their biomass can be used in the production of food, animal feed, bioactive compounds, biofuels and biofertilizers [18]. However, there are few reports about their use as corrosion inhibitors in the literature [12–14,19–22].

Green microalgae of the Chlorella genus are unicellular organisms that have a spherical shape, with no flagella. *Chlorella sorokiniana* is a green microalga that can be grown in fresh or saline water and consumes both inorganic carbon, performing photosynthesis, and organic carbon [23–24]. Therefore, it is a species robust to environmental variations and has rapid growth. Microalgae produce a wide variety of primary biomolecules with potential industrial interest, such as proteins, carbohydrates and lipids, in addition to several intermediate compounds, for example, carotenoids and phycobilins [25].

Our previous works showed that proteins and polysaccharides could be important in inhibiting mild steel corrosion in an acidic medium [6,7,22,26]. The objective of this work was to investigate the effect of biomass from microalgae *Chlorella sorokiniana* against the corrosion of mild steel in 1 mol L^{-1} HCl solution using weight-loss measurements, potentiodynamic polarization curves, electrochemical impedance spectroscopy and surface morphological analysis by scanning electron microscopy. The biomass of *Chlorella sorokiniana* was obtained according to principles of green chemistry.

2. EXPERIMENTAL

2.1 Microalgal culturing

C. sorokiniana strain (LEAF0741) is a member of the microalgae collection of the Laboratório de Estudos Aplicados em Fotossíntese (CMLEAF) at the Federal University of Rio de Janeiro, Brazil. The parent cultures of *C. sorokiniana* were cultured in BBM medium [27], exposed to 120 μmol photons m^{-2} s^{-1} under a 12:12 h photoperiod of light:dark cycle, at 30 ± 2 °C under orbital agitation.

After 7 days of cultivation, cells were continuously transferred to a new culture medium, until the experiments started.

2.2. Mixed experimental design

Cell growth was monitored for 20 days by measuring optical density (OD) at 750 nm and analyzing dry weight. A volume of 3.0 mL were collected in duplicate to determine OD and 15 mL of the culture were collected for filtration and subsequent dry weight analysis. The aliquots were collected up to three days after the culture reached the stationary growth phase. The batches were performed at two different temperatures (25 and 30 ºC ± 2), submitted to a photoperiod of 12 h and irradiance of 100, 200 and 300 μmol photons m^{-2} s^{-1}.

For dry weight analysis, the samples were filtered through a glass fiber filter (0.47 μm pore), using a vacuum pump (Prismatec, model 131), with pressure below 50 mmHg [28]. Before use, the filters were maintained at 400 °C for 4 h, then they were kept at 105 °C until constant weight, and finally stored in a desiccator under vacuum. After filtration, the filters with the samples were kept in an oven at 50 ºC until they reached constant weight. The difference in weight of the filter, before and after filtration, corresponds to dry microalgae biomass. Three replicates were performed under the same culture conditions to evaluate cell growth.

2.3 Microalgal growth

The cell growth was determined for 20 days. Daily, 3 mL algal suspension were collected for optical density analyses at 750 nm (Shimadzu, UV-1800). For cell biomass analyses, 5 mL were filtered (Whatman GF/F). Biomass was determined gravimetrically by obtaining the weight difference of the fiber filter dried at 35 °C to a constant weight before and after filtering microalgae cultures. The maximum specific growth rate (μ) was estimated from the linear coefficient of the equation modeling the exponential portion of the growth curve (Equation 1):

$$\mu\ (d^{-1}) = (\ln(N_2) - ln(N_1))/(t_2 - t_1) \quad (1)$$

Where μ is the specific growth rate, N_2 and N_1 are the optical density of cells and t_2 and t_1 are the growth time in days.

2.4 Chemical characterisation of C. sorokiniana biomass

After choosing the best culture condition, 7 L of culturing were inoculated, and the growth was determined in 750 nm until OD reached 1.0. The culture was centrifuged at 12,100 g for 15 minutes. After centrifugation, the cells were dried at 35 °C to constant weight.

The lipid fraction was obtained by the method of Folch et al. [29], and its quantification was performed by gravimetry, after complete evaporation of solvent. The proteins were extracted according

to the method of Lowry et al. [30], modified as described by Mota et. al. [31]. The quantification of total proteins was done by spectrophotometry at 750 nm using bovine serum albumin as standard. For the determination of total carbohydrates, the method of Dubois et al. [32] was used and its quantification was performed by spectrophotometry at 485 nm using glucose as a standard. Ash content was determined according to the AOAC method [33].

2.5 High Molecular Weight Fraction (HMWF) isolation

The high molecular weight fraction (HMWF) was isolated from the aqueous extract of the biomass using an ultrafiltration process with a specific porous membrane of 3 kDa cut (Millipore - USA). The HMWF was retained on the membrane using a centrifuge rotating at 3500 rpm for 40 minutes. HMWF was stored at –4 °C and lyophilized.

2.6 Gravimetric and electrochemical tests

The specimens were made of mild steel (composition: 0.18% C; 0.30% Mn; 0.04% P; 0.05% S m/m and Fe balance), with approximately 13 cm^2. The mild steel surface was abraded with 100, 320 and 600 mesh sandpapers. Then, the specimens were washed with distilled water, degreased with ethanol and dried in hot air. Both gravimetric and electrochemical tests were performed using 1 mol L^{-1} hydrochloric acid solution as electrolyte which was prepared using 37% hydrochloric acid from Merck Co. (Darmstadt, Germany) and double distilled water.

Gravimetric tests were performed varying immersion time (2 and 24 h) and microalgae biomass concentration (100, 200, 400 and 800 mg L^{-1}). The temperature effect (25, 35, 45, 65 and 85 °C) was evaluated using 200 mg L^{-1} of microalgae biomass in an immersion time of 2 h. All tests were done in triplicate. The corrosion inhibition efficiency (IE%) was obtained using Equation 2 [6].

$$IE(\%) = \frac{W_{corr,0} - W_{corr}}{W_{corr,0}} x\ 100 \quad (2)$$

Where, $W_{corr,0}$ is the corrosion rate (g cm^{-2} h^{-1}) in the absence of the inhibitor and W_{corr} is the corrosion rate in the presence of the inhibitor.

The degree of surface coverage (**θ**) for the study of isotherms was obtained from the corrosion rate with 2 h of immersion using Equation 3.

$$\theta = \frac{W_{corr,0} - W_{corr}}{W_{corr,0}} \quad (3)$$

The apparent activation energy of the system (E_a), kinetic parameter related to W_{corr}, was obtained using Equation 4 [6].

$$\log W_{corr} = \frac{-E_a}{2.303\ RT} + \log A \quad (4)$$

Where, W_{corr} is the corrosion rate (g cm^{-2} h^{-1}), E_a is the apparent activation energy (kJ mol^{-1}), A is the pre-exponential factor, T is the absolute temperature (K) and R is the constant of ideal gases (8.314 J K^{-1} mol^{-1}).

Electrochemical measurements were performed in a conventional cell with three electrodes: mild steel as working electrode, saturated calomel electrode as reference, and a platinum wire with a large surface area as a counter electrode. The experiments were carried out in triplicate, with static solution under natural aeration at 25 ºC. An Autolab PGSTAT 128 N potentiostat/galvanostat controlled by Nova software (version 2.1.2) was used in all electrochemical measurements. Initially, open circuit potential (OCP) was measured during 4000 s to achieve stabilization. The electrochemical impedance tests were performed in the frequency range from 10 kHz to 10 mHz with 10 points *per* decade and amplitude of 10 mV (rms). The impedance measurements were performed on the stable open circuit potential with potentiostatic regulation. After the tests, IE% was calculated according to the Equation 5 [6].

$$IE(\%) = \frac{R_P - R_{P,0}}{R_P} x\ 100 \quad (5)$$

Where, R_P and $R_{P,0}$ are the polarization resistances (Ω cm^2) obtained in the presence and absence of inhibitor, respectively.

The polarization curves were performed with a scan rate equal to 1 mV s^{-1} from −300 mV to +300 mV in relation to the stable open circuit potential. The corrosion current densities were obtained using the Tafel extrapolation method. IE% was calculated according to the Equation 6 [6].

$$IE(\%) = \frac{j_{corr,0} - j_{corr}}{j_{corr,0}} x\ 100 \quad (6)$$

Where, $j_{corr,0}$ and j_{corr} are the corrosion current densities (mA cm^{-2}) in the absence and presence of the inhibitor, respectively.

2.7 Surface analysis

The surface of the specimens used in the morphological analysis was sequentially abraded with 100, 320 and 600 mesh sandpapers. Then, the specimens were washed with distilled water, ethanol and dried in hot air. The specimens were immersed for 2 h in 1 mol L^{-1} HCl solution in the absence and presence of 100 mg L^{-1} of *Chlorella sorokiniana* biomass or its HMWF. After the period, the specimens were washed with distilled water and ethanol, dried in hot air and analyzed by scanning electron microscope Phenom ProX with an acceleration voltage of 20 kV.

3. RESULTS AND DISCUSSION

3.1 Cellular growth of C. sorokiniana and biochemical profile

The combined effects of previously established conditions of temperature and irradiance on cell

growth were investigated by growing the microalga in batch cultures exposed to 300 μmol photons m^{-2} s^{-1} with a 12:12 h photoperiod of light:dark cycle under continuous shaking of 136 rpm, at 25 °C in BBM culture medium [27] (Figure 1). *C. sorokiniana* cell growth was followed by optical density at 750 nm, and by dry weight analysis. The specific growth rate was 0.61 ± 0.08 d^{-1}, and the biomass yield was 2 g L^{-1} in dry biomass. Depending on cultivation conditions, changes occur in the specific growth rate, which is defined as the increase in cell mass per unit time. Intensity, quality and the time period of light affect photosynthesis, which is responsible for producing organic matter, cell division and the growth rate of the organism [34].

Cultures were monitored until the 20th day of growth. The exponential growth phase of *C. sorokiniana* culture was verified until the 5th day of culture, followed by a progressive decline until reaching the stationary phase (Figure 1). A tendency for cultivation to enter the stationary phase on the 15th day of cultivation can be observed. Cells were collected on the 5th and 20th days of cultivation for further biochemical analysis. Based on an investigation of the effect of temperature and irradiance on cellular density, these variables were considered in the experimental design. The design matrix of tested variables and the experimental data are given in Table 1. Six experiments were conducted for 7 days using the mixed tool. According to the results, the cellular density varied between 0.555 and 1.175 under 750 nm. The effect and significance of the variables in cellular density were evaluated using Pareto charts (data not show). From the analysis of the effects of these factors on the cellular density, neither irradiance nor temperature interactions showed a significant effect at the 95% confidence level ($p < 0.05$).

The biochemical composition of the microalgae biomass depends on its type and the environmental factors of the growth conditions during cultivation. Factors such as temperature, light and minerals result in different amounts of biochemical molecules [35].

Table 1. Design matrix of experiments for obtaining *C. sorokiniana* biomass.

Experiment	**Independent variable levels**		**Dependent variable**
	Temperature (°C)	Irradiance (μE m^{-2} s^{-1})	Cellular density (750 nm)
	x_1	x_2	
1	30	100	0.641
2	30	200	0.829
3	30	300	0.897
4	25	100	0.555
5	25	200	1.175
6	25	300	1.132

Information on the chemical composition of algae biomass is important to determine its potential for application in biotechnology. The biochemical composition of the sample, that is, lipids, carbohydrates, and proteins, was studied. Table 2 shows the biochemical profile of the species analyzed in this study in two different stages of growth. *C. sorokiniana* showed significant concentrations of protein on the 20th day of culture, but there was no significant difference in the time

of culture for the carbohydrate content. *C. sorokiniana* produced more lipids on the 5th day of cultivation and the ash content was 14.2% with a significant difference between the periods of cultivation. Roy and Pal [36] showed that the dry biomass of microalgae of the *Chlorella* genus could be 40 to 70% protein. Considering the cultivation time and the biochemical composition, we selected the 20th day of cultivation to obtain the biomass for the electrochemical and gravimetric tests.

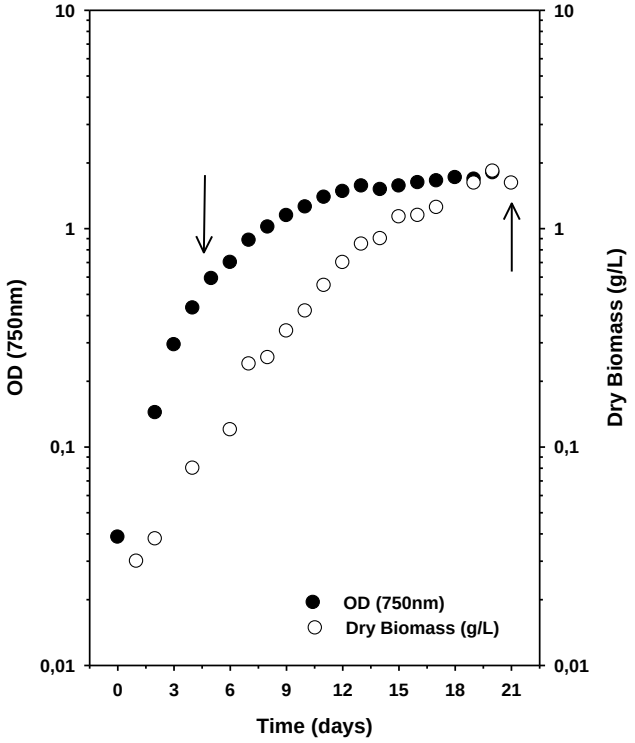

Figure 1. Growth curve of *C. sorokiniana* in BBM medium [27] at 25 °C, 300 µE m^{-2} s^{-1}. Data shown as optical density (●) and dry biomass (○). Arrows indicate culture sampling for analyses.

Table 2. Biochemical composition and ash of dried *C. sorokiniana* biomass (on a dry weight basis).

Composition (%)	**5th day**	**20th day**
Proteins	26.3 ± 2.82^{b}	68.3 ± 5.10^{a}
Carbohydrates	46.2 ± 3.60^{a}	44.1± 5.40^{a}
Lipids	3.05 ± 0.69^{b}	2.14 ± 0.12^{c}
Ash	14.2 ± 0.15^{b}	9.68 ± 0.36^{c}

Mean ± standard deviation (n=3); means in the same row with different superscript letters are significantly different: a > b > c (ANOVA followed by Tukey's post test; $p < 0.05$).

3.2 Weight-loss measurements

3.2.1 Evaluation of inhibitor concentration and immersion time

The weight-loss results of mild steel immersed in 1 mol L^{-1} HCl solution containing different concentrations of microalgae biomass in two immersion times are shown in Table 3. The corrosion rate

decreases and the IE% increases as the inhibitor concentration increases. This result can be explained by the increased coverage of the metal surface by the inhibitor molecules. The inhibition efficiency increases with immersion time, reaching 97.7% of IE after 24 h of exposure to corrosive medium in the presence of 800 mg L^{-1} of biomass. This relationship reveals the stability of the constituent molecules of the biomass of the microalgae *Chlorella sorokiniana* on the metal surface, indicating the existence of a significant interaction between these molecules and the metal surface. Even for the lowest concentration studied in the shortest immersion time, the IE of biomass is high, at 81.0%.

Table 3. Gravimetric results for mild steel immersed in 1 mol L^{-1} HCl solution in the absence and presence of *C. sorokiniana* biomass, at different concentrations and immersion times, at 25 ºC.

Time (h)	[Inhibitor] mg L^{-1}	W_{corr} (g cm^{-2} h^{-1})	IE (%)	SD_{IE} (%)
2	0	$1.21x10^{-3}$	-	-
	100	$2.30x10^{-4}$	81.0	3.3
	200	$1.65x10^{-4}$	86.4	6.2
	400	$1.14x10^{-4}$	90.6	0.7
	800	$8.52x10^{-5}$	93.0	3.6
24	0	$1.68x10^{-2}$	-	-
	100	$9.09x10^{-4}$	94.6	4.3
	200	$4.06x10^{-4}$	97.6	0.2
	400	$4.25x10^{-4}$	97.5	0.1
	800	$3.86x10^{-4}$	97.7	0.4

SD – Standard Deviation.

3.2.2 Adsorption isotherm

To evaluate how the biomass constituents of the microalgae *Chlorella sorokiniana* interact with the metallic surface, calculations were made using four adsorption isotherms (Langmuir, Temkin, Flory-Huggins and El-Awady) that relate the degree of surface coverage (θ) with the inhibitor concentration according to Equations 7–11, respectively. The θ values were calculated from the corrosion rates after 2 h of immersion (data shown in Table 3), according to Equation 3.

$$\frac{C}{\theta} = \frac{1}{K} + C \quad (7)$$

$$\theta = log\left(\frac{-2.303}{2a}\right) + \left(\frac{-2.303}{2a}\right) logC \quad (8)$$

$$log\left(\frac{\theta}{C}\right) = \log K + xlog(1-\theta) \quad (9)$$

$$\log\left(\frac{\theta}{1-\theta}\right) = \log K + y \log C \quad (10)$$

$$\theta = \frac{IE}{100} \quad (11)$$

Where, C is the inhibitor concentration, K is the adsorption constant, a is the lateral interaction parameter between the adsorbed molecules, x is the number of adsorbed water molecules replaced by the inhibitor molecules and y is the number of inhibitor molecules adsorbed in a given active site.

The experimental data best fit to the Langmuir model with R^2 of 0.9999 (Figure 2). Langmuir's model assumes that the inhibitor forms a monolayer on the metallic surface where each active site is occupied by a single molecule of the inhibitor, with no interaction between the molecules of the inhibitor, ie, the sites are equivalent. Note that the angular coefficient of the Langmuir model line was greater than one unit (1.05) (Table 4). This result has been explained in the literature in two ways: it may be due to the interaction between the adsorbed molecules of the inhibitor, or the relationship between the active site for each molecule adsorbed may differ from one unit [6–9].

Temkin, Flory-Huggins and El-Awady models also showed high R^2 values. According to the data found for Temkin isotherm, the parameter a is negative, which indicates that the inhibitor molecules may repel each other. The data obtained from Flory-Huggins and El-Awady isotherms showed $x > 1$ and $y < 1$ revealing that a single inhibitory molecule displaced more than one water molecule and that a single inhibitory molecule occupied more than one active site, showing, in both cases, that the inhibitory molecule is bulky.

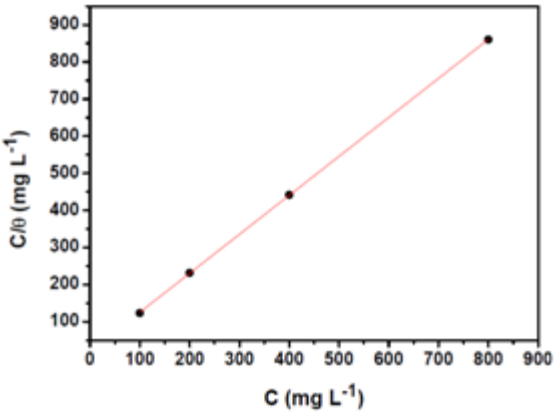

Figure 2. Langmuir isotherm for *C. sorokiniana* biomass on the mild steel surface immersed in 1 mol L^{-1} HCl solution for 2 h immersion time.

Table 4. Data of the Langmuir isotherm obtained by linear adjustment in the experiments with *C. sorokiniana* biomass as inhibitor.

Isotherm	Line Equation	R^2
Langmuir	y = 1.05x + 20.0	0.9999

The results show that the inhibitory molecules present in the biomass of the microalgae *Chlorella sorokiniana* probably adsorbs forming a monolayer. The deviation from Langmuir's behaviour may be due to either the repulsive interaction between the adsorbed molecules or because they are bulky molecules, as evidenced by the data presented in the adjustments of the other isotherms.

3.2.3 Effect of temperature

The effect of temperature on the corrosion of mild steel in 1 mol L^{-1} HCl solution was analyzed. The temperature effect was observed in the absence and presence of 100 mg L^{-1} of biomass of the microalgae after 2 h immersion over a temperature range from 35 to 65 °C. The results of the corrosion rate (W_{corr}) and the inhibition efficiency (IE%) are presented in Table 5.

Table 5. Results obtained after 2 h immersion of mild steel in 1 mol L^{-1} HCl solution in the absence and presence of 100 mg L^{-1} of *Chlorella sorokiniana* biomass, at different temperatures.

Temperature (°C)		**W_{corr} (g cm^{-2} h^{-1})**	***IE* (%)**	**SD_{IE} (%)**
35	Blank	$2.64x10^{-3}$		
	Chlorella sorokiniana	$4.10x10^{-4}$	84.5	0.6
45	Blank	$5.45x10^{-3}$		
	Chlorella sorokiniana	$8.29x10^{-4}$	84.8	3.7
55	Blank	$9.29x10^{-3}$		
	Chlorella sorokiniana	$1.31x10^{-3}$	85.9	1.1
65	Blank	$1.55x10^{-2}$		
	Chlorella sorokiniana	$2.47x10^{-3}$	84.0	3.5

SD – Standard Deviation

The data presented in Table 5 show that the corrosion rate increases both in the absence and in the presence of the inhibitor with increasing temperature. However, there is no significant difference in inhibition efficiency in the studied temperature range. These results show that the increase in temperature does not change the coverage of the metal surface, which leads to the hypothesis that the molecules act only as a blocking inhibitor [37]. The Arrhenius plots, calculated from the data in Table 5, are shown in Figure 3. From the slope of the line in Figure 3A, it is possible to obtain the apparent activation energy associated with the corrosive process of mild steel, according to Equation 4. The activation parameters, ΔH* and ΔS*, were determined by an alternative relation of the Arrhenius equation (Equation 12) [6]:

$$W_{corr} = \frac{RT}{Nh} exp^{\frac{\Delta S*}{R}} exp^{\frac{-\Delta H*}{RT}} \quad (12)$$

Where, h is the Planck constant (6.63 x 10^{-34} J s^{-1}), N is the Avogadro number (6.02 × 10^{23}), ΔS* is the activation entropy and ΔH* is the activation enthalpy.

The plot ln (W_{corr}/T) vs. 1/T (Figure 3B) produces a line equation with the slope of -ΔH*/RT and a linear coefficient of ln (R/Nh) + ΔS*/R, where ΔS* and ΔH* are calculated.

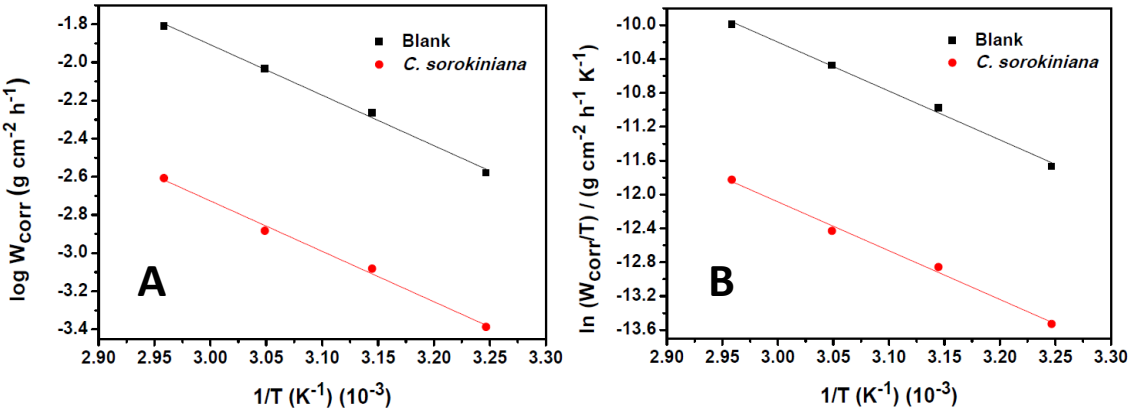

Figure 3. Arrhenius plots: (A) log W_{corr} vs. 1/T; (B) ln (W_{corr}/T) vs. 1/T for mild steel in 1 mol L^{-1} HCl solution in the absence and presence of 100 mg L^{-1} of *Chlorella sorokiniana* biomass.

Table 6. Values of E_a and thermodynamic activation functions (ΔH* e ΔS*) for the corrosion process of mild steel in 1 mol L^{-1} HCl solution in the absence and presence of the microalgae *Chlorella sorokiniana* biomass.

	ΔS* **(J mol^{-1} K^{-1})**	**ΔH*** **(kJ mol^{-1})**	**E_a** **(kJ mol^{-1})**
Blank	–138.4	48.1	50.7
***Chlorella sorokiniana* biomass**	–154.3	48.0	50.6

Table 6 shows the values of the activation parameters (E_a, ΔH* and ΔS*) for the mild steel corrosion process in 1 mol L^{-1} HCl solution in the absence and presence of microalgae biomass. The value of E_a in the absence of the inhibitor is 50.7 kJ mol^{-1} and in the presence of the inhibitor is 50.6 kJ mol^{-1}, which shows that the activation energy does not change in the presence of the inhibitor. Inhibitors that do not change the energy of activation are rare [37]. This phenomenon is verified for the class of blocking inhibitors, where the inhibitor forms a protective film on the metallic surface, thus decreasing the contact surface between the surface and the corrosive medium, consequently decreasing corrosion, without changing the kinetics of the corrosive process.

The positive value of the enthalpy of activation shows that the formation of the activated complex is an endothermic process, and the maintenance of the value with the presence of the inhibitor is a factor that corroborates the hypothesis of inhibition exclusively by blockage. The difference between E_a and ΔH* is equal to RT (2.6 kJ mol^{-1}), which is an indication that the dissolution of the metal is unimolecular. The negative values of ΔS* in the absence (–138.4 J mol^{-1} K^{-1}) and in the

presence (–160.5 J mol^{-1} K^{-1}) of the biomass indicates a stage of association of the activated complex in the determining step.

3.3 Electrochemical experiments

3.3.1 Open circuit potential

The stabilization of the open circuit potential (OCP) was observed with 4000 s of exposure to the blank and in the presence of microalgae biomass (Figure 4).

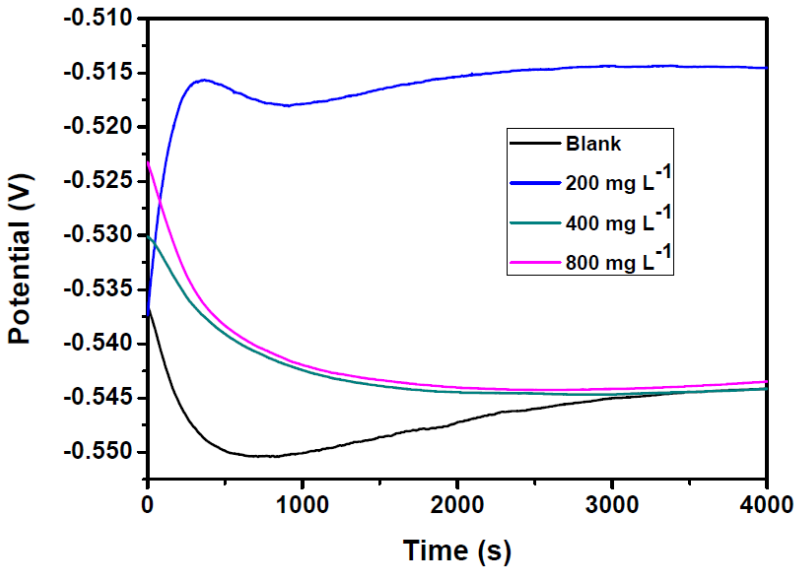

Figure 4. OCP plots for mild steel in 1 mol L^{-1} HCl solution in the absence and in the presence of different concentrations of *Chlorella sorokiniana* biomass.

The OCP stabilized for the blank was −544 mV, while in the presence of the inhibitor it was −543 mV using 800 mg L^{-1} of *Chlorella sorokiniana* biomass, maintaining the same behaviour observed in the absence of inhibitor. There was an anodic shift of 32 mV in the presence of 200 mg L^{-1} of biomass compared to the blank, showing activity as a mixed type inhibitor with an anodic character at open circuit potential.

3.3.2 Potentiodynamic polarization curves

Figure 5 shows the potentiodynamic polarization curves of mild steel in 1 mol L^{-1} HCl solution at concentrations of 200, 400 and 800 mg L^{-1} of *Chlorella sorokiniana* biomass. The electrochemical parameters of corrosion potential (E_{corr}), corrosion current density (j_{corr}), and the anodic (β_a) and cathodic (β_c) constants of Tafel were obtained using the Tafel extrapolation method and are presented in Table 7.

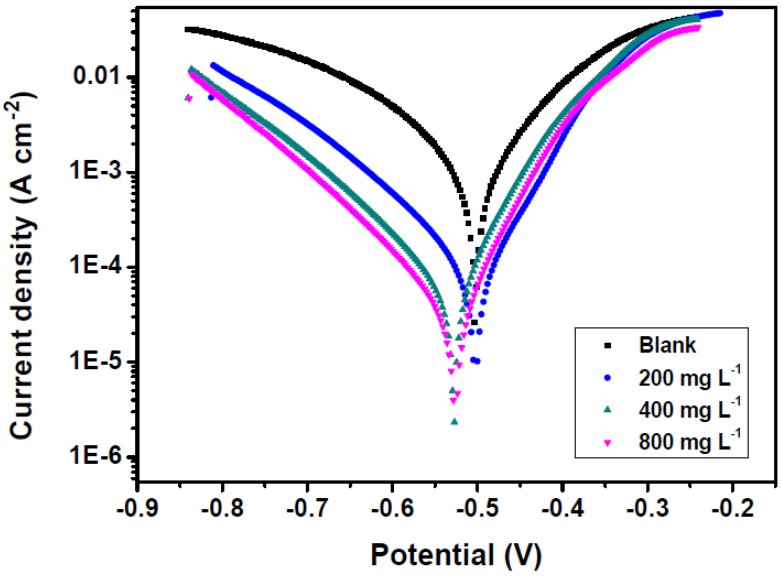

Figure 5. Potentiodynamic polarization curves obtained for mild steel in the absence and presence of different concentrations of *Chlorella sorokiniana* biomass. The total immersion time at which the polarization curves were recorded was 5500 s.

Table 7. Kinetic parameters obtained by Tafel extrapolation method for mild steel in 1 mol L^{-1} HCl solution in the absence and presence of *Chlorella sorokiniana* biomass at different concentrations.

[Inhibitor] (mg L^{-1})	**E_{OCP} (mV)**	**E_{corr} (mV)**	**j_{corr} (mA cm^{-2})**	***-βc* (*mV dec^{-1}*)**	***βa* (*mV dec^{-1}*)**	**IE (%)**
0	–544	–503	$6.45x10^{-1}$	97.2	91.5	-
200	–512	–497	$6.98x10^{-2}$	105	71.8	89.2
400	–544	–528	$7.19x10^{-2}$	125	66.3	88.8
800	–543	–527	$3.35x10^{-2}$	107	59.8	94.8

The inhibition efficiency is enhanced as the inhibitor concentration increases, as in the weight-loss tests. This result shows that the biomass of *Chlorella sorokiniana* acts as an excellent inhibitor of corrosion of mild steel in an acidic medium.

Figure 5 shows a decrease in current density in both the anodic and cathodic process with the addition of the microalgae biomass. This reduction is more clearly expressed in the cathodic branch. In the presence of *Chlorella sorokiniana* biomass, E_{corr} shifted to more negative values, with a displacement of –25 mV and –24 mV using 400 and 800 mg L^{-1} of the inhibitor, respectively. The E_{OCP} did not change with the addition of 400 and 800 mg L^{-1} of microalgae biomass. These results show that polarization influences the adsorption process of inhibitory molecules.

3.3.3 Electrochemical impedance spectroscopy (EIS)

Figure 6A shows the Nyquist diagram in the absence and presence of *Chlorella sorokiniana* biomass at different concentrations. It is possible to observe the appearance of a single capacitive loop in the frequency range used. The capacitive loops are flattened, which is attributed to the surface roughness during the corrosion process [38]. This is also the reason for using the constant phase element (CPE) instead of the electrical double layer capacitance in the data analysis [9,38].

The analysis of all diagrams was based on the equivalent circuit shown in Figure 7 where R_S is the ohmic solution resistance, R_p is the polarization resistance and CPE is the constant phase element. The impedance of the CPE is expressed by Equation 13 [39]:

$$Z_{CPE} = \frac{1}{Y_o(j\omega)^n} \quad (13)$$

Where, Y_0 is the magnitude of CPE and n represents the deviation from the ideal behaviour between –1 and 1, $\omega_{max} = 2\pi f_{max}$ and $j^2 = -1$.

The double layer capacitance, C_{dl}, was calculated using the CPE magnitude, according to the Equation 14 [7]:

$$C_{dl} = Y_o(2\pi f_{max})^{n-1} \quad (14)$$

Where, Y_o is the magnitude of CPE, n represents the deviation from the ideal behaviour, and f_{max} is the frequency at which the imaginary component of the impedance is maximum.

Table 8 shows the parameters obtained from the electrochemical impedance diagrams in different concentrations of the microalgae biomass.

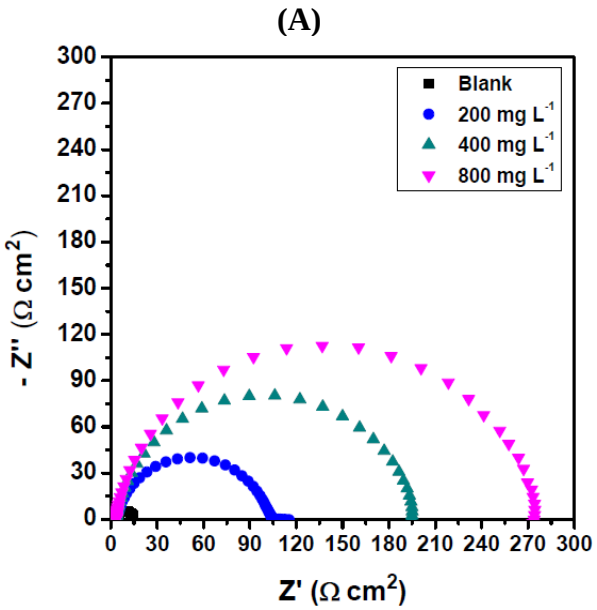

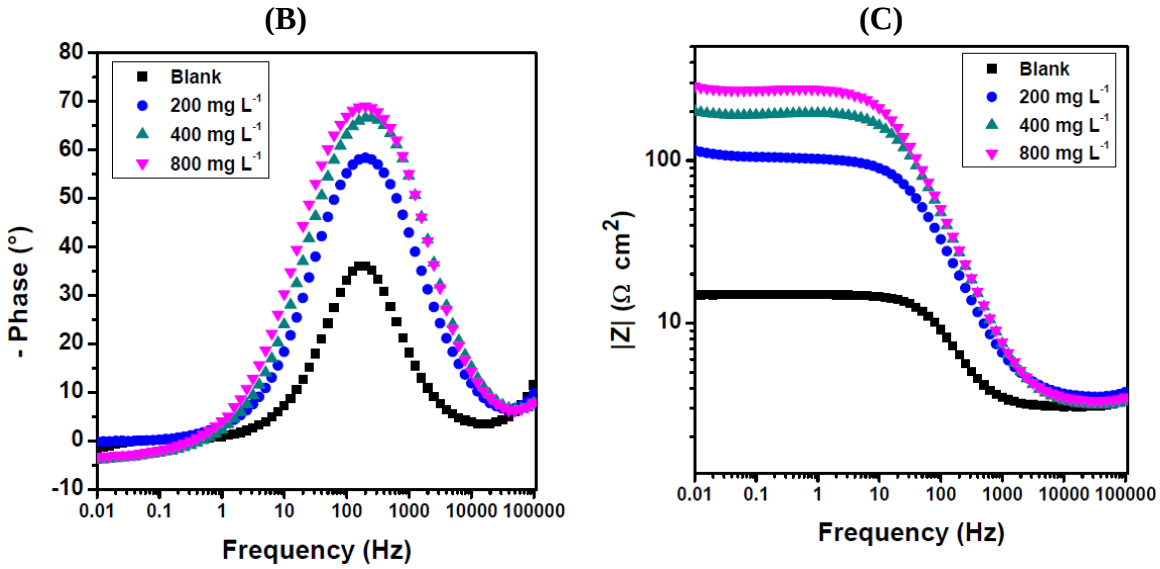

Figure 6. Nyquist diagram (A); and Bode diagrams (B) Phase angle *versus* Frequency; and (C) Impedance module *versus* Frequency for mild steel in 1 mol L^{-1} HCl solution in the absence and in the presence of the inhibitor at different concentrations.

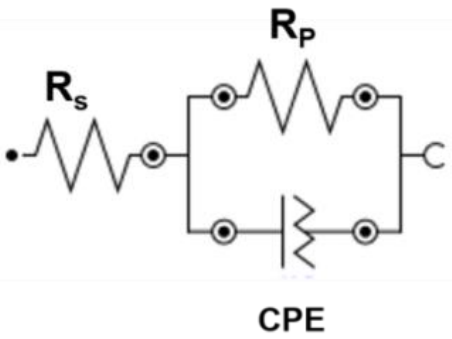

Figure 7. Equivalent circuit proposed for the interpretation of EIS experimental data.

The polarization resistance (R_p) increases significantly with the increment of the inhibitor concentration and f_{max} reduces, causing the decrease of electrical double layer capacitance (C_{dl}), consequently leading to an increase in inhibition efficiency (IE%) values. The inhibition efficiency of 95.5% at the concentration of 800 mg L^{-1} corroborates the weight-loss results previously discussed. The increase in R_p and the decrease in f_{max} in the presence of the inhibitor show that the components present in the biomass modify the structure of the electrical double layer, which suggests that the inhibitor molecules act by adsorption at the metal/solution interface.

Table 8. Electrochemical parameters obtained from EIS technique for mild steel immersed in 1 mol L^{-1} HCl solution in the absence and presence of *Chlorella sorokiniana* biomass at different concentrations.

[Inhibitor] (mg L^{-1})	f_{max} **(Hz)**	R_p **(Ω cm^2)**	Y_o **(μMho s^n cm^{-2})**	C_{dl} **(μF cm^{-2})**	***n***	***IE*** **(%)**
0	79.4	12.0	213	119	0.906	-
200	31.6	102	98.6	45.5	0.854	88.2
400	20.0	191	53.0	31.6	0.893	93.7
800	15.8	270	49.8	31.1	0.898	95.5

As discussed in the Nyquist diagrams, the Bode diagrams show an increase in the values of the phase angle (Figure 6B) and the impedance modulus (Figure 6C), when compared to the blank. In the analyzed frequency range, the diagrams showed a single time constant around 200 Hz.

A blocking-only inhibitor must present values of R_p and j_{corr} constant and equal to the system without an inhibitor, if the effective metal area in contact with the solution is corrected, ie, normalizing this parameter by (1–**θ**), from the weight-loss data with 2 h of immersion. Table 9 shows the R_p values normalized by (1–**θ**). The values of R_p and j_{corr} are practically constant and very close to those of the system without the inhibitor, showing that the inhibitory action of the biomass components is probably exclusively blocking.

Table 9. Normalized R_p and j_{corr} obtained for mild steel immersed in 1 mol L^{-1} HCl solution in the absence and presence of *Chlorella sorokiniana* biomass considering the fraction of the surface not covered by adsorbed molecules (1–θ) from the weight-loss data with 2 h immersion time.

[inhibitor] mg L^{-1}	**θ**	**(1–θ)**	**Normalized R_p (Ω cm^2)**	**Normalized j_{corr} (mA cm^{-2})**
0	-	-	12.0	$6.45x10^{-1}$
200	0.864	0.136	13.9	$5.13x10^{-1}$
400	0.906	0.094	17.9	$7.65\ x10^{-1}$
800	0.930	0.070	18.9	$4.79\ x10^{-1}$

3.4 Surface analysis

Figure 8 shows the morphological analysis of the surface of mild steel before immersion (A), after 2 h of immersion in 1 mol L^{-1} HCl solution (B) and after 2 h of immersion in the acidic solution containing 100 mg L^{-1} of the microalgae biomass (C).

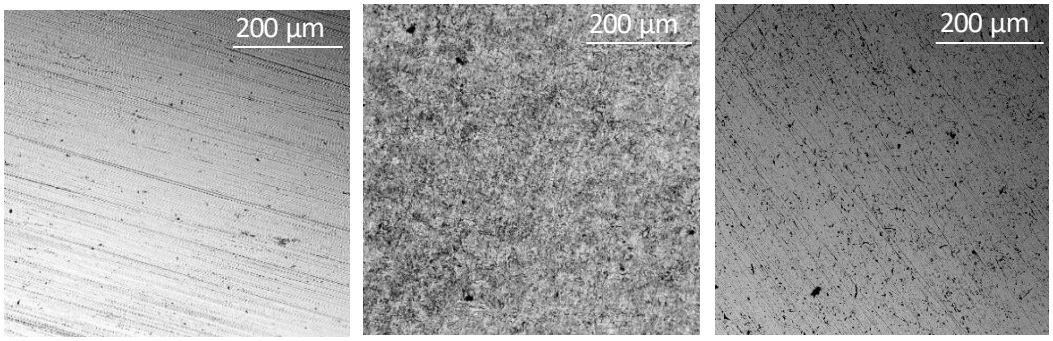

(A) **(B)** **(C)**

Figure 8. SEM micrographs of the mild steel: (A) abraded surface before immersion; (B) specimen immersed in 1 mol L^{-1} HCl solution; (C) specimen immersed in 1 mol L^{-1} HCl solution containing 100 mg L^{-1} of *Chlorella sorokiniana* biomass. The specimens were immersed for 2 h at room temperature. The analyses were made with an acceleration speed of 15 kV and an image increase of 400x.

In the Figure 8B (in the absence of inhibitor), it is possible to observe that the corrosive attack was much more expressive when compared to Figure 8C (in the presence of inhibitor), since the surface presents significant roughness and does not present a uniform aspect. In the Figure 8C, it looks like the abraded specimen, before the corrosive attack. The surface is much less rough and much more uniform when compared to the specimen immersed in the acidic solution without inhibitor. This analysis corroborates the results of weight-loss and electrochemical tests, which show that the *Chlorella sorokiniana* biomass acts as an efficient corrosion inhibitor in the protection of mild steel in 1 mol L^{-1} HCl solution.

3.5 Mechanism

The biomass of *Chlorella sorokiniana* has a significant amount of proteins and carbohydrates, both in its exponential and stationary growth phases, as seen in Table 2. Based on this, gravimetric and electrochemical experiments were carried out using its high molecular weight fraction (HMWF). The same weight-loss experiments, varying inhibitor concentration and immersion time, were performed with the HMWF, and the results are shown in Table 10. The results obtained with the HMWF of *Chlorella sorokiniana* biomass present a behaviour similar to that of total biomass seen in Table 3. This observation leads to the hypothesis that the macromolecules present in the biomass are responsible for the inhibitory action.

Figure 9 shows the results of the polarization curves (A), open circuit potential (B) and electrochemical impedance measurements (C and D) in the absence and presence of 200 mg L^{-1} of microalgae biomass and its HMWF. Table 11 presents the kinetic parameters obtained from anodic and cathodic curves in the absence and presence of 200 mg L^{-1} of the microalgae biomass and its HMWF.

Table 10. Gravimetric assays for mild steel in 1 mol L^{-1} HCl solution in the presence and absence of high molecular weight fraction (HMWF) of *Chlorella sorokiniana* biomass at different concentrations and immersion time.

Time (h)	[Inhibitor] mg L^{-1}	W_{corr} (g cm^{-2} h^{-1})	IE (%)	SD_{IE} (%)
2	0	$1.21x10^{-3}$	-	-
	100	$1.59x10^{-4}$	86.9	0.5
	200	$1.51x10^{-4}$	87.5	0.8
	400	$1.09x10^{-4}$	91.0	2.1
	800	$6.35x10^{-5}$	94.8	0.4
24	0	$1.69x10^{-3}$	-	-
	100	$3.73x10^{-4}$	97.8	0.1
	200	$3.03x10^{-4}$	98.2	0.2
	400	$3.55x10^{-4}$	97.9	0.1
	800	$9.44x10^{-5}$	99.4	0.1

SD – Standard Deviation

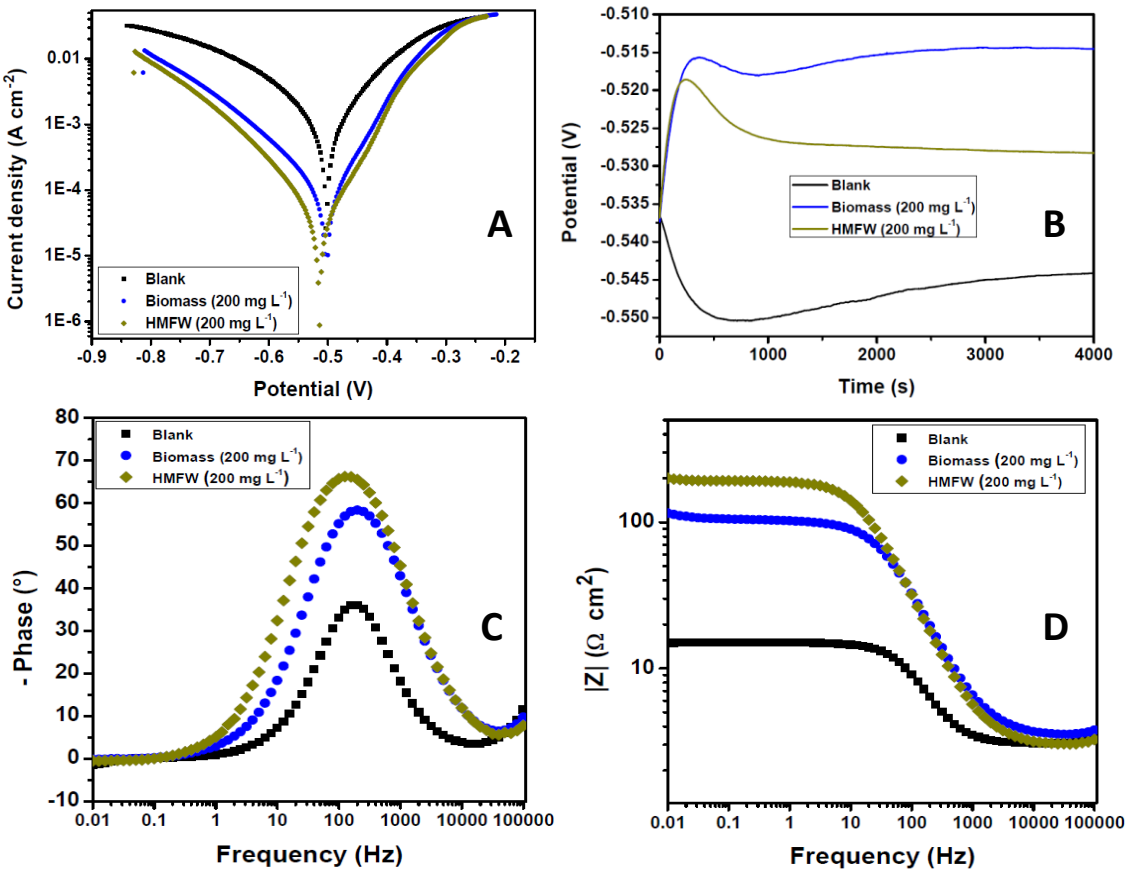

Figure 9. Potenciodynamic polarization curves (A), Open circuit Potential (B) and eletrochemical impedance (C and D) for mild steel in 1 mol L^{-1} HCl solution in the absence and in the presence of 200 mg L^{-1} of *Chlorella sorokiniana* biomass and its high molecular weight fraction.

Table 11. Electrochemical parameters obtained from de anodic and cathodic polarization curves of mild steel in 1 mol L^{-1} HCl solution in the absence and presence of 200 mg L^{-1} of *Chlorella sorokiniana* biomass and its HMWF.

	E_{OCP} (mV)	E_{corr} (mV)	j_{corr} (mA cm^{-2})	$-\beta_c$ ($mV\ dec^{-1}$)	$-\beta_a$ ($mV\ dec^{-1}$)	IE (%)
Blank	–544	–503	$6.45x10^{-1}$	97.2	91.5	-
Total biomass	–512	–497	$6.98x10^{-2}$	105	71.8	89.2
HMWF	–531	–515	$4.18x10^{-2}$	94.3	67.3	93.5

Table 11 shows that the HMWF obtained inhibition efficiency very close to the biomass. Therefore, the HMWF has a fundamental part in the inhibitory action of the microalgae *Chlorella sorokiniana* because it presents high inhibition efficiency when compared to the absence of an inhibitor. The parameters obtained from the impedance diagrams in the absence and presence of 200 mg L^{-1} of the biomass of *Chlorella sorokiniana* and its HMWF are shown in Table 12.

Table 12. Electrochemical parameters obtained from the impedance diagrams of mild steel immersed in 1 mol L^{-1} HCl solution in the absence and presence of 200 mg L^{-1} of *Chlorella sorokiniana* biomass and its HMWF.

	f_{max} (Hz)	R_p ($\Omega\ cm^2$)	Y_o ($\mu Mho\ s^n\ cm^{-2}$)	C_{dl} ($\mu F\ cm^{-2}$)	*n*	*IE* (%)
Blank	79.4	12.0	213	119	0.906	-
Total biomass	31.6	102	98.6	45.5	0.854	88.2
HMWF	12.6	190	44.1	26.2	0.881	93.7

The impedance diagram (Figure 9C) shows a single capacitive loop in the presence of 200 mg L^{-1} of the HMWF, as observed with the total microalgae biomass. HMWF has greater polarization resistance than biomass, which consequently increases the inhibition efficiency, indicating that macromolecules are fundamental to the inhibitory action of *Chlorella sorokiniana* biomass.

Figure 10 shows the morphological analysis of the surface of mild steel after immersion for 2 h in 1 mol L^{-1} HCl solution containing 100 mg L^{-1} of HMWF from *Chlorella sorokiniana* biomass. It is possible to observe a very similar behaviour to that seen in the presence of 100 mg L^{-1} of the total biomass of the microalgae (Figure 8C), showing again that the macromolecules play an important role in the inhibitory action of the biomass, as also seen with the biomass of *Spirulina maxima* [22].

The biomass of *Chlorella sorokiniana* showed an IE% value higher than that found for the biomass of the microalgae *Spirulina maxima* in our previous work [22]. In the presence of 200 mg L^{-1} of *Chlorella sorokiniana* biomass, 86.4, 89.2 and 88.2% IE were obtained from the results of corrosion rate with 2 h of immersion, corrosion current density and polarization resistance, respectively. The biomass of *Spirulina maxima* presented 68.5, 73.3 and 67.9% IE in the same conditions [22]. Although both microalgae have a high protein content, *Chlorella sorokiniana* biomass proved to be an even more effective inhibitor than *Spirulina maxima* biomass.

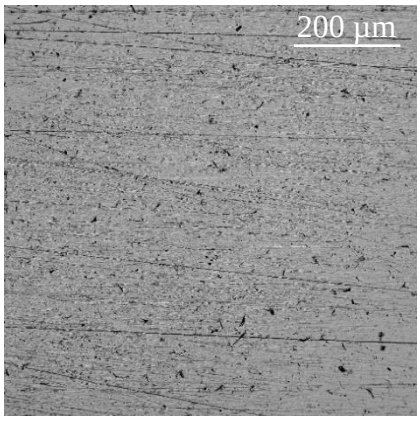

Figure 10. SEM micrograph of the mild steel immersed for 2 h in 1 mol L^{-1} HCl solution containing 100 mg L^{-1} of HMWF from *Chlorella sorokiniana* biomass.

4. CONCLUSION

The biomass of the microalgae *Chlorella sorokiniana* proved to be an excellent corrosion inhibitor of mild steel in 1 mol L^{-1} HCl solution. The macromolecules have a fundamental contribution to the inhibitory action of biomass because the high molecular weight fraction presents inhibition efficiency higher than the total biomass.

The apparent activation energy did not change with the addition of the inhibitor which characterizes adsorption by blocking, where the molecules present in the microalgae biomass form a protective film on the metallic surface of mild steel. The adsorption of the inhibitor followed the Langmuir isotherm, which admits the formation of a monolayer of the inhibitor molecules on the metal surface. The values of R_P and j_{corr} were normalized by $(1-\theta)$, being θ obtained by gravimetric experiments. The normalized values were very close to the blank test, corroborating the hypothesis that the biomass components act purely as a blocking inhibitor. The SEM analysis showed that the biomass and its HMWF keep the metal surface much less rough in the presence of the inhibitor, due to the adsorption of the macromolecules that slows down the corrosive process of mild steel.

ACKNOWLEDGMENTS
The authors thank CNPq (Conselho Nacional de Desenvolvimento Científico e Tecnológico) for financial support (process number 424306/2016-6 and 312005/2018-0). The authors are also thankful to CNPq for the scholarship for V.M.Teixeira. The authors would like to thank Núcleo de Desenvolvimento de Processos e Análises Químicas em Tempo Real – NQTR – IQ/UFRJ for SEM analysis.

References

1. V. Gentil, Corrosão, LTC Livros Técnicos e Científicos Editora S.A., (1996) Rio de Janeiro, Brazil.
2. G. Koch, J. Varney, N. Thompson, O. Moghissi, M. Gould and J. Payer, International Measures of Prevention, Application, and Economics of Corrosion Technologies Study, NACE Int., (2016) Houston, USA.

3. P. B. Raja, M. Ismail, S. Ghoreishiamiri, J. Mirza, M. C. Ismail, S. Kakooei and A. A. Rahim, *Chem. Eng. Commun*., 203 (2016) 1145.
4. Z. Tang, *Curr. Opin. Solid State Mater. Sci.,* 23 (2019) 100759.
5. S. Varvara, R. Bostan, O. Bobis, L. Găină, F. Popa, V. Mena and R. M. Souto, *Appl. Surf. Sci*., 426 (2017) 1100.
6. C. A. Santana, J. N. da Cunha, J. G. A. Rodrigues, J. Greco-Duarte, D. M. G. Freire and E. D'Elia, *J. Braz. Chem. Soc*., 31 (2020) 1225.
7. R. F. B. Cordeiro, A. J. S. Belati, D. Perrone and E. D'Elia, *Int. J. Electrochem. Sci*., 13 (2018) 12188.
8. É. C. dos Santos, R. Cordeiro, M. dos Santos, P. R. P. Rodrigues, A. Singh and E. D'Elia, *Mater. Res*., 22 (2019) 1.
9. R. S. Trindade, M. R. dos Santos, R. F. B. Cordeiro and E. D'Elia, *Green Chem. Lett. Rev*., 10 (2017) 444.
10. V. M. Teixeira, E. Santos, M. J. C. Rezende and E. D'Elia, *Rev. Virtual Quim*., 7 (2015) 1780.
11. L. A. C. Matos, M. C. Taborda, G. J. T. Alves, M. T. da Cunha, E. P. Banczek, M. F. Oliveira, E. D'Elia and P. R. P. Rodrigues, *Int. J. Electrochem. Sci*., 13 (2018) 1577.
12. G. G. P. de Souza, M. T. G. de Sampaio, A. B. Furtado, P. H. M. Buzzetti, C. J. B. Ramos, V. L. Teixeira, J. A. C. Velasco, R. N. Damasceno and E. A. Ponzio, *Rev. Virtual Quim*., 11 (2019) 1521.
13. T. Benabbouha, R. Nmila, M. Siniti, K. Chefira, H. El Attari and H. Rchid., *SN Appl. Sci.,* 2 (2020) 1.
14. R. Thilagavathi, A. Prithiba and R. Rajalakshmi, *Orient. J. Chem*., 35 (2019) 241.
15. S. Aribo, S. J. Olusegun, L. J. Ibhadiyi, A. Oyetunji and D. O. Folorunso, *J. Assoc. Arab Univ. Basic Appl. Sci.,* 24 (2017) 34.
16. Y. Shirmohammadli, D. Efhamisisi and A. Pizzi, *Ind. Crops Prod*., 126 (2018) 316.
17. L. S. Berlim, A. G. Bezerra Jr., W. M. Pazin, T. S. Ramin, W. H. Schreiner and A. S. Ito, *J. Lumin*., 194 (2018) 394.
18. A. León-Vaz, R. León, E. Díaz-Santos, J. Vigara and S. Raposo, *N. Biotechnol*., 51 (2019) 31.
19. Y. Abboud , A. Abourriche , T. Ainane , M. Charrouf , A. Bennamara , O. Tanane and B. Hammouti, *Chem. Eng. Commun*., 196 (2009) 788.
20. D. K. Verma and F. Khan, *Green Chem. Lett. Rev*., 9 (2016) 52.
21. M. Ramdani, H. Elmsellem, N. Elkhiati, B. Haloui, A. Aouniti, M. Ramdani, Z. Ghazi, A. Chetouani and B. Hammouti, *Der Pharma Chem*., 7 (2015) 67.
22. L. S. Rodrigues, A. F. do Valle and E. D'Elia, *Int. J. Electrochem. Sci*., 13 (2018) 6169.
23. A. M. Lizzul, P. Hellier, S. Purton, F. Baganz, N. Ladommatos and L. Campos, *Bioresour. Technol.,* 151 (2014) 12.
24. L. Ramanna, A. Guldhe, I. Rawat and F. Bux, *Bioresour. Technol*., 168 (2014) 127.
25. A. Maadane, N. Merghoub, T. Ainane, H. El Arroussi, R. Benhima, S. Amzazi, Y. Bakri and I. Wahby, *J. Biotechnol*., 215 (2015) 13.
26. E. C. C. A. de Souza, B. A. Ripper, D. Perrone and E. D'Elia, *Mater. Res*., 19 (2016) 1276.
27. R. A. Andersen, Algal Culturing Techniques, Elsevier Academic Press, (2005) San Diego, USA.
28. J. C. Goldman and M. R. Dennett, *J. Exp. Mar. Bio. Ecol*., 86 (1985) 47.
29. J. Folch, M. Lees and G. H. S. Stanley, *J. Biol. Chem*., 226 (1957) 497.
30. O. H. Lowry, N. J. Rosebrough, A. L. Farr, R. J. Randall, *J. Biol. Chem*., 193 (1951) 265.
31. M. F. S. Mota, M. F. Souza, E. P. Bon, M. A. Rodrigues and S. P. Freitas, *J. Phycol*., 54 (2018) 577.
32. M. Dubois, K. Gilles, J. K. Hamilton, P. A. Rebers and F. Smith, *Nature,* 168 (1951) 167.
33. AOAC. Official methods of analysis of the association of official analytical chemists international, AOAC International, (2000), 17th ed., Gaithersburg, USA.
34. D. P. K. Nogueira, A. F. Silva, O. Q. F. Araújo and R. M. Chaloub, *Biomass Bioenergy*, 72 (2015) 280.
35. M. R. Brown, S. W. Jeffrey, J. K. Volkman and G. A. Dunstan, *Aquaculture*, 151 (1997) 315.

36. S. S. Roy and R. Pal, *Proc. Zool. Soc*., 68 (2015) 1.
37. Y. I. Kuznetsov, N. N. Andreev and S. S. Vesely, *Int. J. Corros. Scale Inhib*., 4 (2015) 108.
38. V. V. Torres, V. A. Rayol, M. Magalhães, G. M. Viana, L. C. S. Aguiar, S. P. Machado, H. Orofino and E. D'Elia, *Corrosion Sci*., 79 (2014) 108.
39. C. H. Hsu and F. Mansfeld, *Corrosion*, 57 (2001) 747